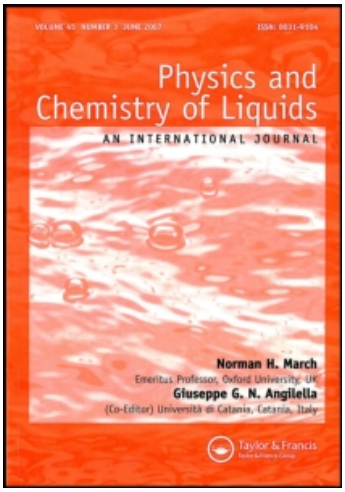

Physics and Chemistry of Liquids
Publication details, including instructions for authors and subscription information:
http://www.informaworld.com/smpp/title~content=t713646857

The Electron Liquid-Solid Phase Transition In Two Dimensions in a Magnetic Field

M. J. Lea[a]; N. H. March[b]
[a] Department of Physics, Royal Holloway & Bedford New College, University of London, Surrey, England [b] Theoretical Chemistry Department, University of Oxford, Oxford, England

To cite this Article Lea, M. J. and March, N. H.(1990) 'The Electron Liquid-Solid Phase Transition In Two Dimensions in a Magnetic Field', Physics and Chemistry of Liquids, 21: 3, 183 — 193
To link to this Article: DOI: 10.1080/00319109008028482
URL: http://dx.doi.org/10.1080/00319109008028482

Phys. Chem. Liq., 1990, Vol. 21, pp. 183–193
Reprints available directly from the publisher
Photocopying permitted by licence only

THE ELECTRON LIQUID-SOLID PHASE TRANSITION IN TWO DIMENSIONS IN A MAGNETIC FIELD

M. J. LEA* and N. H. MARCH†

* *Department of Physics, Royal Holloway & Bedford New College, (University of London), Egham, Surrey, TW20 0EX. England.*

† *Theoretical Chemistry Department, University of Oxford, 5, South Parks Road, Oxford, OX1 3UB. England.*

(Received 27 October 1989)

We present a simple model for the melting curve of a two-dimensional electron solid in a magnetic field and compare it with recent experiments on the phase diagram of 2-D electrons on cryogenic substrates and in GaAs/GaAlAs heterojunctions.

KEY WORDS: Wigner crystallisation, Landau filling factor, melting temperature.

1 INTRODUCTION

Some 50 years ago Wigner[1] proposed that at sufficiently low density the delocalized electron liquid in jellium would give way to a localized electron crystal. The physical reason for this, as he clearly recognized, was that at low density where the potential energy dominates the kinetic contribution to the total energy E, the electrons would avoid each other maximally by going on to the sites of a lattice—the Wigner crystal. The lattice with the lowest Madelung energy is body-centered-cubic (bcc) and most probably this will exhibit long-range antiferromagnetic order[2,3], the upward spins occupying one of the two interpenetrating simple cubic lattices and the downward spins the other.

Unfortunately, it has, to date, not proved possible to simulate Wigner's electron crystal in the laboratory, though quantum Monte Carlo calculations[4] on the jellium model have fully vindicated Wigner's ideas on the electron liquid-electron crystal phase transition. However, in 1968, Durkan, Elliott and March[5] proposed an interpretation of the Hall effect data of Putley[6] on n-type InSb in a magnetic field in terms of Wigner crystallization taking place at a critical value of the applied magnetic field. Subsequent experiments by Somerford[7] on the same system were interpreted by Care and March[8] as a Wigner transition aided by the magnetic field. Later, Kleppmann and Elliott[9,10] pressed this interpretation and showed that the anisotropy of the conductivity measured by Somerford was consistent with the Wigner transition. More recently, McDonald and Bryant[11] have recalculated the energy of a 3-D

electron plasma in a magnetic field including a precise treatment of the exchange energy. They find a phase diagram with several other types of ground state ordering besides the simple electron Wigner crystal, depending on the field strength and the density.

Very recently, interest in the magnetically induced Wigner solid (MIWS) has been revived by the beautiful experiments of Andrei *et al.*[12] and Glattli *et al.*[13] on a 2-D electron assembly in a GaAs/GaAlAs heterojunction. These workers pointed out that a crucial difference between an electron liquid (delocalized state) and an electron solid is that only the latter can sustain low frequency shear waves. Evidence was given by Andrei *et al.*[12] that their 2-D electrons, in a magnetic field, could support shear waves. Though an alternative interpretation of the experimental data of Andrei *et al.* has been suggested by Stormer and Willett,[14] the experiments have now been repeated and the MIWS provides the most probable explanation of the data. The sharp onset of a propagating mode was used to plot the phase diagram for Wigner crystallisation as a function of temperature and field.

The purpose of this paper is to present a simple model of two-dimensional Wigner crystallisation and its melting curve to an electron liquid phase in an applied magnetic field. This model will then be compared with experiments in both classical and quantum 2-D electron solids.

2 THE WIGNER OSCILLATOR MODEL

The model incorporates, in a phenomenological way, the quantum effects of zero-point motion, the Kosterlitz-Thouless melting criterion and some aspects of the anharmonicity of the electron lattice vibrations. The work of March and Tosi[15] on a localised harmonic oscillator in a magnetic field is taken as the starting point. They calculated the canonical matrix for this system which reduces to the result for free electrons of Sondheimer and Wilson[16] as the oscillator force constant tends to zero. The Landau energy levels for free electrons in a magnetic field of arbitrary strength are embodied fully in this limit. With non-zero force constant for the localised oscillator, the energy levels calculated by Darwin[17] are involved in the calculation of the canonical density matrix and therefore of its trace which is essentially the partition function.

The idea behind the present work is then simply stated. Each electron is taken as oscillating in a harmonic potential well produced by the other electrons in the Wigner crystal. This is an Einstein model including field dependent zero point motion. The mean square displacement $\langle r^2 \rangle$ in the plane will be field and temperature dependent and can be calculated from the canonical density matrix $C(\boldsymbol{r}, \beta)$ as

$$\langle r^2 \rangle = \frac{\int r^2 C(\boldsymbol{r}, \beta) \mathrm{d}\boldsymbol{r}}{\int C(\boldsymbol{r}, \beta) \mathrm{d}\boldsymbol{r}} \tag{1}$$

where $\beta = 1/kT$. This calculation[18] gives

$$\langle r^2 \rangle = \frac{\hbar}{m\omega_L b F(\alpha, b)} \tag{2}$$

where ω_L is the Larmor frequency $eH/2mc$,

$$F(a, b) = \coth(b\alpha) - \frac{\cosh(\alpha)}{\sinh(b\alpha)} \tag{3}$$

and $\alpha = \hbar\omega_L/kT$. The parameter b is given by

$$b = (1 + \omega_W^2/\omega_L^2)^{1/2} \tag{4}$$

where ω_W is the natural frequency of the localised Wigner oscillator, which will be close to the characteristic phonon frequency ω_0 given by Bonsall and Maradudin[19] as $\omega_0^2 = 8e^2/ma^3$.

It is convenient to work in terms of the reduced variables $t = T/T_{mc}$ where T_{mc} is the melting temperature of the classical crystal, the Landau level filling factor $\nu = nhc/eH$ and $r_s = r_0/a_B$ where $r_0 = (\pi n)^{-1/2}$ in 2 dimensions. Eq. (2) then becomes

$$\frac{\langle r^2\rangle}{a^2} = \frac{(\sqrt{3}/2\pi)\nu}{bF(\alpha, b)} = \frac{0.276\nu}{bF(\alpha, b)}$$

$$\text{with } \alpha = \frac{\Gamma_m}{\nu r_s t}; \qquad b = (1 + D\nu^2 r_s)^{1/2} \tag{5}$$

and we have assumed a triangular lattice for the 2-D crystal. The only free parameter is the constant $D = 1.158\,(\omega_W/\omega_L)^2$ which defines the natural frequency of the Wigner oscillators. It is instructive to consider the limiting forms of eq. (5). For $r_s \gg 1$, in the classical limit

$$\frac{\langle r^2\rangle}{a^2} = \frac{0.552t}{\Gamma_m D} \tag{6}$$

and this result is also obtained in the high field limit, $\nu = 0$, for all values of r_s. Thus, as is well known, a magnetic field suppresses the zero-point motion and produces a classical 2-D crystal. At $t = 0$, the only contribution to $\langle r^2\rangle$ comes from the zero-point motion in which the quantum limit, $r_s = 0$, is given by

$$\begin{aligned}\langle r^2\rangle/a^2 &= 0.276\nu \\ &= 2l_B^2/a^2\end{aligned} \tag{7}$$

where $l_B = hc/eH$ is the magnetic length. For $r_s \gg 1$ at $t = 0$ we have the zero-point motion of the 2-D oscillator

$$\langle r^2\rangle/a^2 = \frac{0.276}{(Dr_s)^{1/2}} \tag{8}$$

In this model $\langle r^2\rangle$ is defined with respect to a lattice point in the crystal. But in 2-D $\langle r^2\rangle$ diverges logarithmically[20] as the overall crystal size increases to infinity, due to low frequency acoustic modes. However, this does not prevent the formation of a crystal as the relevant parameter is the mean relative displacement of nearest neighbours defined as

$$\langle (r_i - r_{i+1})^2\rangle/a^2 = \gamma \tag{9}$$

and called the mean melting parameter by Lozovik *et al.*[21] For our Einstein model we have

$$\gamma = \langle r_i^2 \rangle / a^2 + \langle r_{i+1}^2 \rangle / a^2 - \langle 2 r_i r_{i+1} \rangle / a^2$$
$$= 2\langle r^2 \rangle / a^2 \tag{10}$$

since the motion of neighbouring electrons is uncorrelated.

There is strong experimental evidence[22] that the melting of a 2-D classical crystal is a Kosterlitz-Thouless (K-T) transition due to the thermal unbinding of dislocation pairs when the shear modulus μ is given by

$$\mu = 4\pi k T / a^2. \tag{11}$$

Hence the melting temperature T_{mc} of a 2-D classical crystal is

$$T_{mc} = \frac{e^2}{r_0 k \Gamma_m} \tag{12}$$

where $\Gamma_m = 127 \pm 3$, as determined experimentally for electrons on helium.[23]

In order to apply the K-T criterion to our general model we require a relationship between μ and the parameter γ. In the classical limit the shear modulus decreases with temperature (for $t \ll 1$) as

$$\mu^* = \mu / \mu_0 = 1 - Ct \tag{13}$$

where μ_0 is the zero temperature modulus and C has been measured experimentally[23] as 0.3 ± 0.1. Computer simulations by Morf[24] (which gave $C = 0.23$) and Bedanov *et al.*[25] and calculations by Lozovik *et al.*[21] strongly suggest that the decrease in μ is due to anharmonicity of the electron lattice. However, this anharmonicity seems to have much less effect on γ which increases almost linearly with temperature,[25] as eq. (6) until the K-T transition intervenes at $\gamma = \gamma_c = 0.03$. In this classical limit this Lindemann melting criterion and the K-T transition both lead to a melting temperature T_{mc} as given in eq. (12). We can use this result to determine the vibrational parameter $D = 1.104/\gamma_c \Gamma_m = 0.292$ in our model eq. (5). In the high density, quantum limit at $T = 0$ the K-T transition is suppressed (i.e. only occurs when μ falls to zero) and μ will continue to decrease as $\gamma = 0.552v$ increases beyond γ_c. Lozovik *et al.*[21] have calculated μ and γ versus v in this limit and found that μ decreased and γ increased almost linearly until the crystal became unstable at $v = v_q$ (0.126 in their calculations) due to anharmonicity.

Combining the classical and quantum results we therefore assume that, in general,

$$\mu^* = 1 - A\gamma(r_s, H, T); \gamma \leq \gamma_q$$
$$= \mu_1 \qquad ; \gamma = \gamma_q$$
$$= 0 \qquad ; \gamma \geq \gamma_q \tag{14}$$

where γ is given by eqs. (10) and (5), until $\gamma = \gamma_q$ at $\mu^* = \mu_1$ when the crystal becomes unstable. Glattli *et al.*[13] found that the low temperature limit of their postulated Wigner crystal occurred for $v = v_q = 0.192$ which is equivalent to $\gamma_q = 0.106$ and we

use this value. Hence the only free parameter in our model is μ_1. Even this is tightly constrained since, in eq. (13), $C = (1 - \mu_1)\gamma_c/\gamma_q$ and hence for $C = 0.23$[24], $\mu_1 = 0.19$ while for $C = 0.3 \pm 0.1$[22] we find $\mu_1 = -0.06 \pm 0.35$.

Finally, from eqs. (11) and (14) the 2-D melting temperature t_m is given by

$$t_m = \frac{1 - A\gamma(r_s, H, T)}{1 - A\gamma_c}; \gamma \leq \gamma_q$$
$$= 0 \qquad ; \gamma > \gamma_q \tag{15}$$

For $\gamma < \gamma_q$ this will be a K-T transition while for $\gamma = \gamma_q$ the transition could be driven by an anharmonic instability in the lattice vibrations, though other mechanisms could be invoked. Note that eq. (15) is not equivalent to a pure Lindemann criterion since γ_m, the value at the melting point, is

$$\gamma_m = t_m\gamma_c + (1 - t_m)\gamma_0 \tag{16}$$

where $\gamma_0 = 1/A$. Our model corresponds to a temperature dependent γ_m.

At finite temperatures we should also consider the thermally excited modes in the crystal. In a magnetic field the longitudinal plasmon mode $\omega_p(q)$ and the transverse phonon mode $\omega_t(q)$ are transformed to two magnetophonon modes $\omega_\pm(q)$ where

$$\omega_+^2 = \omega_c^2 + \omega_p^2 + \omega_t^2; \omega_- = \omega_p\omega_t/\omega_c. \tag{17}$$

In a complementary approach to the one taken in this paper Saitoh[26] calculated $\langle r^2 \rangle$ from the excitation of these collective ω_+ and ω_- modes, and used the Lindemann criterion to obtain the melting curve. The Einstein model gives qualitatively similar results, though Saitoh's calculations predict larger quantum effects at relatively low electron densities.

In high fields $\omega_c \gg \omega_p$, the zero-point energy is contained in the ω_+ mode, close to the cyclotron frequency. It is this motion that has been treated quantum-mechanically in the Einstein model above. The low frequency transverse ω_- mode will be thermally excited for

$$\frac{\hbar\omega_-}{kT} \approx \frac{\hbar\omega_c}{kT}\left(\frac{\omega_0}{\omega_c}\right)^2 \approx \frac{\Gamma_m \nu}{2t} < 1 \tag{18}$$

where ω_c is the cyclotron frequency. It was the propagation of the ω_- mode which Andrei *et al.*[12] used as the criterion for a solid. But this mode will only contribute thermally to $\langle r^2 \rangle$ for $\nu < 0.02t$ in the high field classical limit. It would then give a term proportional to T but since eq. (5) already provides such a term in this limit no extra contribution from the ω_- mode is required.

Figure 1 shows a schematic phase diagram in the t-ν plane for several values of r_s. In the classical low density limit, $r_s \to \infty$, the melting temperature is independent of magnetic field. As the density increases the zero field melting temperature decreases. In the quantum limit, $r_s \to 0$, the phase diagram is independent of density and the melting temperature has its classical value for $\nu = 0$. As ν increases t_m decreases, but remains a K-T transition until $\gamma = \gamma_q$ when some other instability occurs at $\nu = 0.192$

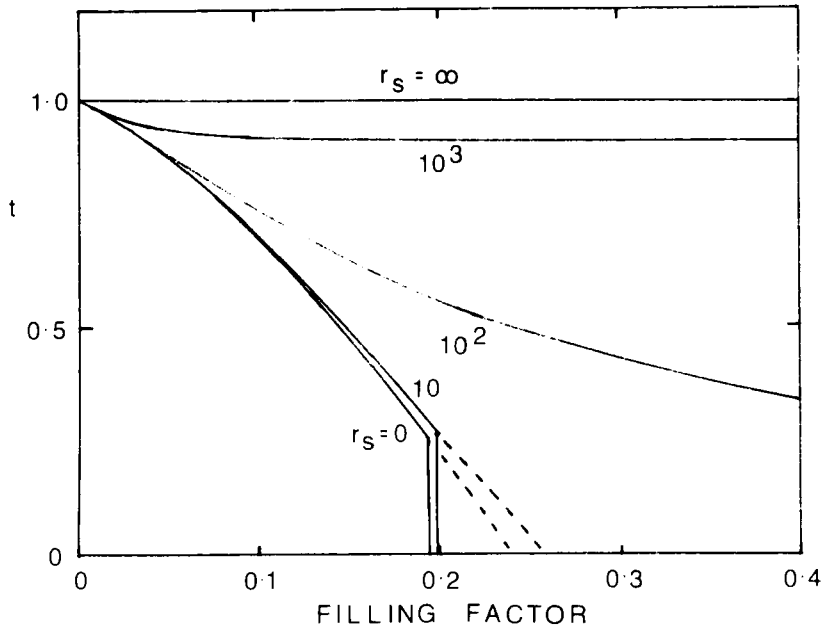

Figure 1 Schematic phase diagram of the 2-D electron solid for several values of r_s.

for the parameters used here. The dashed lines show the extrapolation of the K-T transition.

We will now compare this simple model with experiments on classical and quantum 2-D electron solids.

2.1. *The classical 2-D electron solid*

It is well established that in the classical, or low density limit, $r_s = \infty$, the melting temperature equals T_{mc}, eq.(12), for a K-T transition with $\Gamma_m = 127 \pm 3$ [23]. A magnetic field should have no effect on the thermodynamics of a classical solid and T_m should be independent of H.[28,29] However, at high densities T_m should be less than T_{mc}. These effects have been calculated by several authors,[26–31] notably by Chang and Maki,[29] Fisher[28] and Saitoh[26] though the results vary considerably.

Saitoh[26] calculated γ for the longitudinal and transverse magnetoplasmons in the 2-D crystal and used the modified Lindemann criterion $\gamma = \gamma_m = 0.03$ to obtain the phase diagram for all densities. His results predict relatively large increases in $T_m(B)$ with magnetic field at densities which are easily accessible for electrons on helium. Chang and Maki[29] calculated the shear modulus, allowing for anharmonicity, for all densities in zero field. In the classical region, $r_s > 300$ they found that the small quantum corrections increased μ, i.e. stiffened the crystal, and hence $T_m(0) > T_{mc}$ though the effect was small. Fisher[28] calculated the shear modulus for a high density crystal in the high-field, or classical, limit and also found an initial increase in $T_m > T_{mc}$ as the field is reduced from infinity.

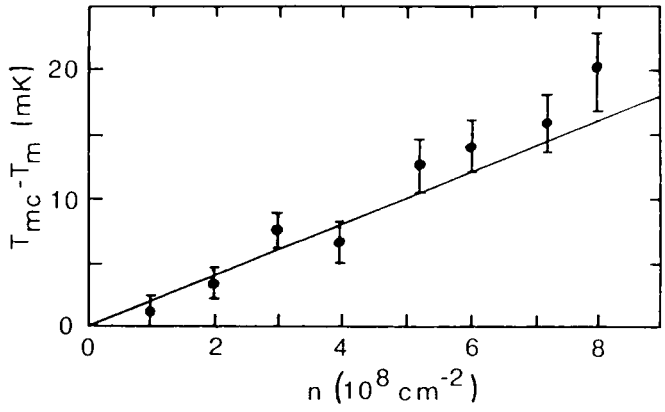

Figure 2 The experimental data of Mehrotra *et al.*[32] for 2-D electrons on helium showed a decrease in the melting temperature in zero field below the classical result Eq. (12). The solid line shows the model calculations.

Our model is equivalent to a temperature dependent Lindemann criterion, eq. (16), and hence will always give $T_m < T_{mc}$ though the magnitude of the quantum corrections will be less than the pure Lindemann criterion used by Saitoh.

Experimentally, the situation is unclear. In zero field Mehrotra, Guenin and Dahm[32] found a decrease in T_m below T_{mc} for electrons on helium for $n < 8 \times 10^8$ cm^{-2} as shown in Figure 2. The solid line shows the quantum corrections calculated from our model with $\mu_1 = 0.2$, which are in good agreement with the experiments. No quantum corrections to T_m were reported by Kono[33] or Deville[22] for $n < 12 \times 10^8$ cm^{-2} for electrons on helium or by Kajita[34] for $n < 2 \times 10^{10}$ cm^{-2} for electrons on solid neon, though in each case the measured T_m and the predicted quantum corrections are within the error bars.

Recently, Stone *et al.*[35] have measured the field dependence of T_m for electrons on helium for $n = 8.1 \times 10^8$ cm^{-2} as shown in Figure 3. They found that T_m was almost independent of field, possibly decreasing slightly to 7 T. These results are in better agreement, within the error bars, with the theories of Fisher[28] and Chang and Maki[29] than with the simple model presented here.

However, both the experiments and theory are difficult and subtle in this region. The main conclusion is that quantum effects are small and difficult to compute or observe in the experimentally accessible region for electrons on cryogenic substrates.

2.2. *The quantum 2-D crystal*

The 2-D electron assembly has been extensively studied in Si MOSFET's and in GaAl/GaAlAs heterostructures. In zero magnetic field these systems are in the high density limit and the electrons form a Fermi degenerate gas. As the magnetic field is increased, the Integer and Fractional Quantum Hall effects are observed.[36] The latter is characterized by a series of new ground states of the electron fluid, which is providing a wealth of new Physics. At the highest fields, for $\nu < 0.2$, Andrei *et al.*[12] and

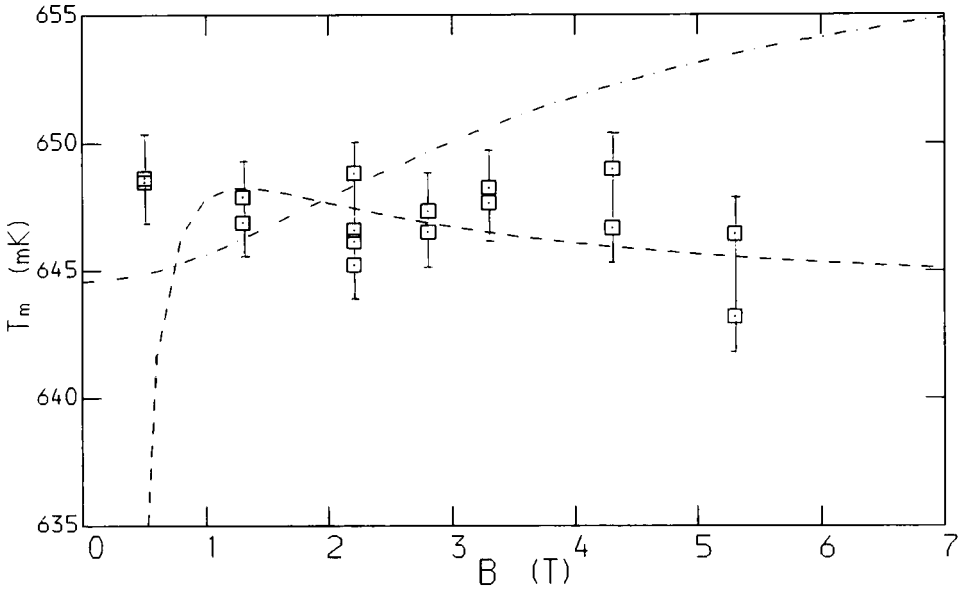

Figure 3 The experimental data of Stone *et al.*[35] for 2-D electrons on helium, $n = 8.1 \times 10^8$ cm^{-2}, showed that T_m was almost independent of magnetic field from 0.5 to 7*T*. The dashed line shows the calculation of Fisher[28] (with $T_{mc} = 643.5$ mK) while the dot-dashed line shows the result of the model used here (with $T_{mc} = 662$ mK).

Glattli *et al.*[13] have reported the probable occurrence of the MIWS for $\nu < \nu_q = 0.192 \pm 0.004$. The electron density for these experiments gives $1.6 < r_s < 2.5$. The experimental solid-fluid transitions t_m in the t-ν plane are shown in Figure 4. The data for many densities is shown and while the error bars are quite large, the general shape of the phase diagram is clear.

For $r_s \leq 5$, our model calculations suggest that, on a t-ν plot, the phase diagram corresponds to the quantum limit and is independent of density. The model phase diagram is shown in Figure 4 for $\mu_1 = 0.2$ (line a) and 0 (line b). For $\mu_1 = 0$ the transition remains of the K-T type down to the lowest temperatures. However, a better fit to the data is obtained for $\mu_1 = 0.2$ with a sharp drop in t_m at $\nu_q = 0.192$. Thus the transition would be of K-T type for $t_m > 0.24$, but some other form of crystalline instability would occur at lower temperatures. In a real system the detailed form of the phase diagram near ν_q would depend on the increasing anharmonicity and the nature of the excitations and ground state of the solid and fluid phases.

In the high field limit, $\nu \to 0$, the transition temperature of the ideal 2-D system should tend to T_{mc}. But at high electon densities the finite extent of the wave functions perpendicular to the 2-D plane will modify the Coulomb interaction[37] and should reduce t_m by a factor of about 0.87.[12] With this in mind the model phase diagram agrees reasonably well with the data.

This model can also be used to calculate the phase diagram for intermediate values of r_s, a region not yet accessible experimentally. A key parameter here is the limiting

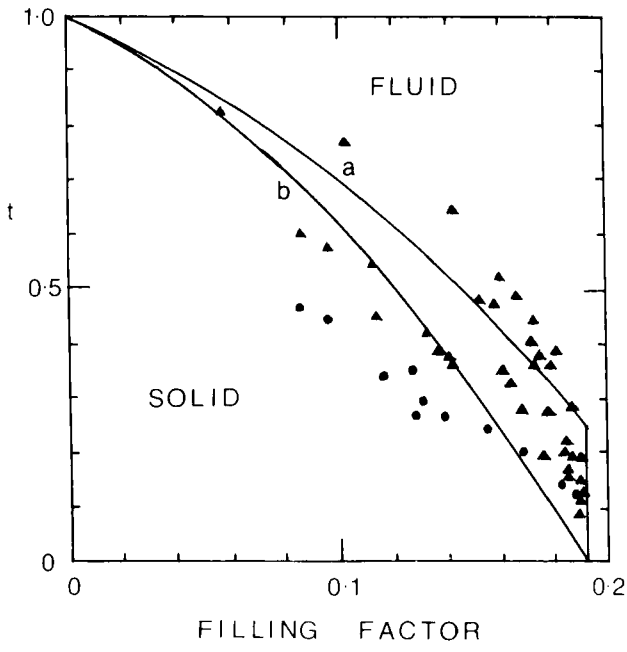

Figure 4 The experimental data of Andrei *et al.*[12] (o) and of Glattli *et al.*[13] (Δ) for 2-D electrons in GaAs/GaAlAs heterostructures. The points represent the onset of a new mode in the response of the electron gas which was interpreted as a phase transition to an MIWS. The solid lines show the model phase diagram for $\mu_1 = 0.2$ (line a) and $\mu = 0$ (line b).

value of $r_s = r_W$ at which the 2-D Wigner solid in stable in zero magnetic field. For our model that is given by

$$r_W = \frac{0.276\gamma_c\Gamma_m}{\gamma_q^2} \tag{20}$$

and has the value 93 for the parameters used. This has not yet been measured experimentally though a wide range of values have been found theoretically[27,25] from 4.5 to 1400. Probably the best estimate, $r_W = 33$, comes from the computer simulations of Ceperley[30] and Imada and Takahashi[31]. In this region an Einstein model may be less valid as the zero-point motion of the propagating plasmons will determine $\langle r^2 \rangle$ and the crystal could remain stable to higher densities.

It is interesting to speculate on the existence of the 2-D hexatic phase on this phase diagram. In the classical limit, Nelson and Halperin[38] argued that the K-T transition should be from a solid to an orientationally-ordered phase with the transition to a true fluid occurring at a temperature $t_1 \geq 1$. This hexatic phase has not yet been observed experimentally, though a transition in viscosity was found by Frankel and McTague[39] in a computer simulation, at $t_1 = 1.58$. Since the $\nu = 0$ phase diagram in the high density limit is the same as the classical one, this phase should also be present. Other phases of the fluid or solid could also exist.

SUMMARY

In 2-D a simple phenomenological model has been presented as a framework for discussion of the experiments on the 2-D classical electron solid on helium and neon and on the MIWS in GaAs/GaAlAs heterostructures. The parameters of the model are determined, within close limits, by results from computer simulations and experiments. While it is not expected to be fully quantitative it does give a guide to the phase diagram in both the classical and quantum regions.

The similarity between the results of Andrei *et al.*[12] and Glattli *et al.*[13] and the model developed in the present paper lends strong support to their claim that quantum-mechanical electron solidification has occurred in their experiment, aided by a magnetic field. Much more sophisticated theoretical approaches[5,13,27–31,40] have been used for aspects of this problem and may be generalised in the future. Many other types of ground state order could also be present in the phase diagram besides the simplest electron solid discussed here.

As for further experimental studies, propagation of shear waves establishes an electron solid, but not longer range order. Bragg diffraction studies are still needed to establish crystallinity for the Wigner solid in semiconductors, as has been done using ripplons for the 2D classical solids of electrons on helium[41] and of positive ions below the helium surface.[42]

References

1. E. P. Wigner (1934), *Phys. Rev.* **46**, 1002; *Trans. Faraday Soc.* **34**, 678 (1938).
2. W. J. Carr (1961), *Phys Rev.* **122**, 1437.
3. F. Herman and N. H. March (1984), *Solid State Commun.* **50**, 725.
4. D. M. Ceperley and B. J. Alder (1980), *Phys. Rev. Lett.* **45**, 566.
5. J. Durkan, R. J. Elliott and N. H. March (1968), *Rev. Mod. Phys.* **40**, 812.
6. E. H. Putley (1960), *Proc. Phys. Soc.* (London) **76**, 802.
7. D. J. Somerford (1971), *J. Phys.* **C4**, 1570.
8. C. M. Care and N. H. March (1971), *J. Phys.* **C4**, L372.
9. W. G. Kleppmann and R. J. Elliott (1975), *J. Phys.* **C8**, 2729.
10. R. J. Elliott and W. Kleppmann (1975), *J. Phys.* **C8**, 2737.
11. A. H. McDonald and G. W. Bryant (1987), *Phys. Rev. Letts.* **58**, 515.
12. E. Y. Andrei, G. Deville, D. C. Glattli, F. I. B. Williams, E. Paris and B. Etienne (1988), *Phys. Rev. Lett.* **60**, 2765.
13. D. C. Glattli, G. Deville, V. Duburcq, F. I. B. Williams, E. Paris, B. Etienne and E. Y. Andrei, Proc. 8th *Intern. conf. on Electron Prop. of 2-D Systems*, Surface, Science. In Press.
14. H. L. Stormer and R. L. Willett (1989), *Phys Rev. Lett.*, **62**, 972.
15. N. H. March and M. P. Tosi (1985), *J. Phys.* **A18**, L643.
16. E. H. Sondheimer and A. H. Wilson (1951), *Proc. Roy. Soc.* **A 210**, 173.
17. C. G. Darwin (1931), *Proc. Camb. Phil. Soc.* **27**, 86.
18. N. H. March and M. P. Tosi (1985), *Nuovo Cimento* **6D**, 521.
19. L. Bonsall and A. A. Maradudin (1977), *Phys. Rev. B.* **15**, 1959.
20. N. D. Mermin (1968), *Phys Rev.* **176**, 250.
21. Yu. E. Lozovik, V. M. Fartztdinov and B. Abdullaev (1985), *J. Phys. C.* **18**, L807.
22. G. Deville (1988), *J. Low Temp. Phys.* **72**, 135.
23. F. Gallet, G. Deville, A. Valdes and F. I. B. Williams (1982), *Phys Rev. Letts.* **48**, 212; G Deville, A. Valdes, E. Y. Andrei and F. I. B. Williams (1984), *Phys. Rev. Letts.* **53**, 588.
24. R. H. Morf (1979), *Phys. Rev. Letters* **43**, 931.
25. V. M. Bedanov, G. V. Gadiyak and Yu. E. Lozovik (1985), *Phys. Lett.* **109A**, 289.

26. M. Saitoh (1988), *Surf. Sci.* **196**, 8.
27. P. M. Platzman and H. Fukuyama (1974), *Phys. Rev. B* **10**, 3150.
28. D. S. Fisher (1982), *Phys. Rev. B* **26**, 5009.
29. M. Chang and K. Maki (1983), *Phys. Rev. B* **27**, 1646.
30. D. Ceperley (1978), *Phys. Rev. B* **18**, 3126.
31. M. Imada and M. Takahashi (1984), *J. Phys. Soc. Japan*, **53**, 3770.
32. R. Mehrotra, B. M. Guenin and A. J. Dahm (1982), *Phys. Rev. Letts.* **48**, 641.
33. K. Kono (1987), *J. Phys. Soc. Japan* **56**, 1111.
34. K. Kajita (1985), *J. Phys. Soc. Japan*, **54**, 4092.
35. A. O. Stone, M. J. Lea, P. Fozooni and J. Frost: *J. Phys. CM.* In Press.
36. K. von Klitzing, G. Dorda and M. Pepper (1980), *Phys Rev. Lett.* **45**, 494; D. C. Tsui, H. L. Stormer and A. C. Gossard (1982), *Phys. Rev. Lett.* **48**, 1559; R. B. Laughlin (1983), *Phys. Rev. Lett.* **50**, 1395.
37. F. C. Zhang and S. Das Sarma (1986), *Phys. Rev. B* **33**, 2903.
38. D. R. Nelson and B. I. Halperin (1979), *Phys. Rev.* **19**, 2457.
39. D. Frenkel and J. P. McTague (1979), *Phys. Rev. Letts.* **42**, 1632.
40. K. Maki and X. Zotos (1983), *Phys Rev. B* **28**, 4349; P. K. Lam and S. M. Girvin (1984), *Phys. Rev. B* **30**, 473; D. Levesque, J. J. Weis and A. H. MacDonald (1984), *Phys. Rev. B* **30** 1056; S. T. Chui, T. M. Hakim and K. B. Ma (1986), *Phys. Rev. B* **33**, 7110; S. Kivelson, C. Kallin, D. P. Arovas and J. R. Schrieffer (1987), *Phys. Rev. B.* **36**, 1620.
41. C. C. Grimes and G. Adams (1979), *Phys. Rev. Lett.* **42**, 795.
42. C. J. Mellor and W. F. Vinen, *Proc 8th Intern. Conf. on Electronic Properties of 2-D Systems*, Surface Science. In Press.